

# Causal Generative Neural Networks

Olivier Goudet\*<sup>1</sup>, Diviyan Kalainathan\*<sup>1</sup>, Philippe Caillou<sup>1</sup>, Isabelle Guyon<sup>1</sup>,  
David Lopez-Paz<sup>2</sup>, Michèle Sebag<sup>1</sup>

<sup>1</sup>TAU, CNRS – INRIA – LRI, Univ. Paris-Sud, Univ. Paris-Saclay

<sup>2</sup>Facebook AI Research

## Abstract

We present Causal Generative Neural Networks (CGNNs) to learn functional causal models from observational data. CGNNs leverage conditional independencies and distributional asymmetries to discover bivariate and multivariate causal structures. CGNNs make no assumption regarding the lack of confounders, and learn a differentiable generative model of the data by using backpropagation. Extensive experiments show their good performances comparatively to the state of the art in observational causal discovery on both simulated and real data, with respect to cause-effect inference, v-structure identification, and multivariate causal discovery.

## 1 Introduction

Deep learning models have shown tremendous predictive abilities in image classification, speech recognition, language translation, game playing, and much more [Goodfellow *et al.*, 2016]. However, they often mistake correlation for causation [Stock and Cisse, 2017], which can have catastrophic consequences for agents that plan and decide from observation.

The gold standard to discover causal relations is to perform experiments [Pearl, 2003]. However, whenever experiments are expensive, unethical, or impossible to realize, there is a need for *observational causal discovery*, that is, the estimation of causal relations from observation alone [Spirtes *et al.*, 2000; Peters *et al.*, 2017]. In observational causal discovery, some authors exploit distributional asymmetries to discover bivariate causal relations [Hoyer *et al.*, 2009; Zhang and Hyvärinen, 2009; Daniusis *et al.*, 2012; Stegle *et al.*, 2010; Lopez-Paz *et al.*, 2015; Fonollosa, 2016], while others rely on conditional independence to discover structures on three or more variables [Spirtes *et al.*, 2000; Chickering, 2002]. Different approaches rely on different but equally strong assumptions, such as linearity [Shimizu *et al.*, 2006], additive noise [Zhang and Hyvärinen, 2009; Peters *et al.*, 2014], determinism [Daniusis *et al.*, 2012], or a large corpus of annotated causal relations [Lopez-Paz *et al.*, 2015; Fonollosa, 2016]. Among the most promising approaches are

score-based methods [Chickering, 2002], assuming the existence of external *score-functions* that must be powerful enough to detect diverse causal relations. Finally, most methods are not differentiable, thus unsuited for deep learning pipelines.

The ambition of **Causal Generative Neural Network (CGNNs)** is to provide a unified approach. CGNNs learn functional causal models (Section 2) as generative neural networks, trained by backpropagation to minimize the Maximum Mean Discrepancy (MMD) [Gretton *et al.*, 2007; Li *et al.*, 2015] between the observational and the generated data (Section 3). Leveraging the representational power of deep generative models, CGNNs account for both distributional asymmetries and conditional independencies, tackle the bivariate and multivariate cases, and deal with hidden variables (confounders). They estimate both the causal graph underlying the data and the full joint distribution, through the architecture and the weights of generative networks. Unlike previous approaches, CGNNs allow non-additive noise terms to model flexible conditional distributions. Lastly, they define differentiable joint distributions, which can be embedded within deep architectures. Extensive experiments show the state-of-the-art performance of CGNNs (Section 4) on cause-effect inference, v-structure identification, and multivariate causal discovery with hidden variables.<sup>1</sup>

## 2 The language of causality: FCMs

A Functional Causal Model (FCM) upon a random variable vector  $X = (X_1, \dots, X_d)$  is a triplet  $C = (\mathcal{G}, f, \mathcal{E})$ , representing a set of equations:

$$X_i \leftarrow f_i(X_{\text{Pa}(i;\mathcal{G})}, E_i), E_i \sim \mathcal{E}, \text{ for } i = 1, \dots, d \quad (1)$$

Each equation characterizes the direct causal relation from the set of causes  $X_{\text{Pa}(i;\mathcal{G})} \subset \{X_1, \dots, X_d\}$  to observed variable  $X_i$ , described by some *causal mechanism*  $f_i$  up to the effects of noise variable  $E_i$  drawn after distribution  $\mathcal{E}$ , accounting for all unobserved phenomenon. For simplicity,  $X_i$  interchangeably denotes an observed variable and a node in graph  $\mathcal{G}$ . There exists a direct causal relation from  $X_j$  to  $X_i$ , written  $X_j \rightarrow X_i$ , iff there exists a directed edge from  $X_j$  to

\*Joint first author (firstname.lastname@lri.fr). Rest of authors ordered alphabetically.

<sup>1</sup>Code available at <https://github.com/GoudetOlivier/CGNN>. Datasets available at <http://dx.doi.org/10.7910/DVN/3757KX> and <http://dx.doi.org/10.7910/DVN/UZMB69>.

$X_i$  in  $\mathcal{G}$ . In the following, we restrict ourselves to considering Directed Acyclic Graph (DAG)  $\mathcal{G}$  (Fig. 1) and  $\mathcal{E}$  is set to the uniform distribution on  $[0, 1], U[0, 1]$ .

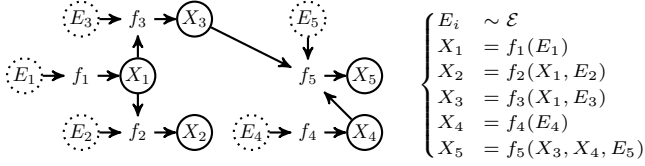


Figure 1: Example FCM for  $X = (X_1, \dots, X_5)$ .

## 2.1 Generative models and interventions

The generative model associated to FCM  $(\mathcal{G}, f, \mathcal{E})$  proceeds by first drawing  $e_i \sim \mathcal{E}$  for all  $i = 1, \dots, d$ , then in topological order of  $\mathcal{G}$  computing  $x_i = f_i(x_{\text{Pa}(i; \mathcal{G})}, e_i)$ .

Importantly, the FCM supports interventions, that is, freezing a variable  $X_i$  to some constant  $v_i$ . The resulting joint distribution noted  $P_{\text{do}(X_i=v_i)}(X)$ , called *interventional distribution* [Pearl, 2009], can be computed from the FCM by discarding all causal influences on  $X_i$  and clamping its value to  $v_i$ . It is emphasized that intervening is different from conditioning (*correlation does not imply causation*). The knowledge of interventional distributions is essential for e.g., public policy makers, wanting to estimate the overall effects of a decision on a given variable.

## 2.2 Formal background and notations

In this section, we introduce notations and definitions and prove the representational power of FCMs.

Two random variables  $(X, Y)$  are *conditionally independent* given  $Z$  if  $P(X, Y|Z) = P(X|Z)P(Y|Z)$ . Three random variables  $(X, Y, Z)$  form a v-structure iff  $X \rightarrow Z \leftarrow Y$ . The random variable  $Z$  is a confounder (or common cause) of the pair  $(X, Y)$  if  $(X, Y, Z)$  have causal structure  $X \leftarrow Z \rightarrow Y$ . The skeleton  $\mathcal{U}$  of a DAG  $\mathcal{G}$  is obtained by replacing all the directed edges in  $\mathcal{G}$  by undirected edges.

Discovering the causal structure of a random vector is a difficult task in all generality. For this reason, the literature in causal inference relies on a set of common assumptions [Pearl, 2003]. The *causal sufficiency* assumption states that there are no unobserved confounders. The *causal Markov* assumption states that all the d-separations in the causal graph  $\mathcal{G}$  imply conditional independences in the observational distribution  $P$ . The *causal faithfulness* assumption states that all the conditional independences in the observational distribution  $P$  imply d-separations in the causal graph  $\mathcal{G}$ . A *Markov equivalence class* denotes the set of graphs with same set of d-separations.

### Proposition 1. Representing joint distributions with FCMs

Let  $X = (X_1, \dots, X_d)$  denote a set of continuous random variables with joint distribution  $P$ , and further assume that the joint density function  $h$  of  $P$  is continuous and strictly positive on a compact subset of  $\mathbb{R}^d$ , and zero elsewhere. Letting  $\mathcal{G}$  be a DAG such that  $P$  can be factorized along  $\mathcal{G}$ ,

$$P(X) = \prod_i P(X_i | X_{\text{Pa}(i; \mathcal{G})})$$

there exists  $f = (f_1, \dots, f_d)$  with  $f_i$  a continuous function with compact support in  $\mathbb{R}^{|\text{Pa}(i; \mathcal{G})|} \times [0, 1]$  such that  $P(X)$  equals the generative model defined from FCM  $(\mathcal{G}, f, \mathcal{E})$ .

*Proof.* By induction on the topological order of  $\mathcal{G}$ , taking inspiration from [Carlier et al., 2016]. Let  $X_i$  be such that  $|\text{Pa}(i; \mathcal{G})| = 0$  and consider the cumulative distribution  $F_i(x_i)$  defined over the domain of  $X_i$  ( $F_i(x_i) = \text{Pr}(X_i < x_i)$ ).  $F_i$  is strictly monotonous as the joint density function is strictly positive therefore its inverse, the quantile function  $Q_i : [0, 1] \mapsto \text{dom}(X_i)$  is defined and continuous. By construction,  $Q_i(e_i) = F_i^{-1}(e_i)$  and setting  $Q_i = f_i$  yields the result.

Assume  $f_i$  be defined for all variables  $X_i$  with topological order less than  $m$ . Let  $X_j$  with topological order  $m$  and  $Z$  the vector of its parent variables. For any noise vector  $e = (e_i, i \in \text{Pa}(j; \mathcal{G}))$  let  $z = (x_i, i \in \text{Pa}(j; \mathcal{G}))$  be the value vector of variables in  $Z$  defined from  $e$ . The conditional cumulative distribution  $F_j(x_j|Z=z) = \text{Pr}(X_j < x_j|Z=z)$  is strictly continuous and monotonous wrt  $x_j$ , and can be inverted using the same argument as above. Defining  $f_j(z, e_j) = F_j^{-1}(z, x_j)$  yields the result.  $\square$

## 3 Causal generative neural networks

Let  $X = (X_1, \dots, X_d)$  denote a set of continuous random variables with joint distribution  $P$ . Under same conditions as in Proposition 1, ( $P(X)$  being decomposable to graph  $\mathcal{G}$ , with continuous and strictly positive joint density function on a compact in  $\mathbb{R}^d$  and zero elsewhere), it is shown that there exists a generative neural network called **CGNN** (Causal Generative Neural Network), that approximates  $P(X)$  with arbitrary accuracy.

### 3.1 Approximating continuous FCMs with CGNN

Firstly, given  $\mathcal{G}$ , it is shown that there exists a set of networks  $\hat{f} = (\hat{f}_1, \dots, \hat{f}_d)$  such that the generative model  $\hat{P}$  defined by  $\hat{X}_i = \hat{f}_i(\hat{X}_{\text{Pa}(i; \mathcal{G})}, E_i)$  with  $E_i \sim \mathcal{E}$  defines a joint distribution arbitrarily close to  $P$ .

**Proposition 2.** For  $m \in [[1, d]]$ , let  $Z_m$  denote the set of variables with topological order less than  $m$  and let  $d_m$  be its size. For any  $d_m$ -dimensional vector of noise values  $e^{(m)}$ , let  $z_m(e^{(m)})$  (resp.  $\hat{z}_m(e^{(m)})$ ) be the vector of values computed in topological order from  $f$  (resp.  $\hat{f}$ ). For any  $\epsilon > 0$ , there exists a set of networks  $\hat{f}$  with architecture  $\mathcal{G}$  such that

$$\forall e^{(m)}, \|z_m(e^{(m)}) - \hat{z}_m(e^{(m)})\| < \epsilon \quad (2)$$

*Proof.* By induction on the topological order of  $\mathcal{G}$ . Let  $X_i$  be such that  $|\text{Pa}(i; \mathcal{G})| = 0$ . Following the universal approximation theorem [Cybenko, 1989], as  $f_i$  is a continuous function over a compact of  $\mathbb{R}$ , there exists a neural net  $\hat{f}_i$  such that  $\|f_i - \hat{f}_i\|_\infty < \epsilon/d_1$ . Thus Eq. 2 holds for the set of networks  $\hat{f}_i$  for  $i$  ranging over variables with topological order 0.

Let us assume that Prop. 2 holds up to  $m$ , and let us assume for brevity that there exists a single variable  $X_j$  with topological order  $m+1$ . Letting  $\hat{f}_j$  be such that  $\|f_j - \hat{f}_j\|_\infty < \epsilon/3$  (based on the universal approximation property), letting  $\delta$

be such that for all  $u$   $\|\hat{f}_j(u) - \hat{f}_j(u + \delta)\| < \epsilon/3$  (by absolute continuity) and letting  $\hat{f}_i$  satisfying Eq. 2 for  $i$  with topological order less than  $m$  for  $\min(\epsilon/3, \delta)/d_m$ , it comes:  $\|(z_m, f_j(z_m, e_j)) - (\hat{z}_m, \hat{f}_j(\hat{z}_m, e_j))\| \leq \|z_m - \hat{z}_m\| + |f_j(z_m, e_j) - \hat{f}_j(z_m, e_j)| + |\hat{f}_j(z_m, e_j) - \hat{f}_j(\hat{z}_m, e_j)| < \epsilon/3 + \epsilon/3 + \epsilon/3$ , which ends the proof.  $\square$

### 3.2 Scoring metric

The architecture and the network weights are trained and optimized using a score-based approach [Chickering, 2002]. The ideal score, to be minimized, is the distance between the joint distribution  $P$  associated with the ground truth FCM, and the joint distribution  $\hat{P}$  defined by the estimated  $(\hat{\mathcal{G}}, \hat{f}, \mathcal{E})$ . A tractable approximation thereof is given by the Maximum Mean Discrepancy (MMD) [Gretton *et al.*, 2007] between the  $n$ -sample observational data  $\mathcal{D}$ , and an  $n$ -sample  $\hat{\mathcal{D}}$  sampled after  $\hat{P}$ . Overall,  $\hat{C}$  is trained by minimizing

$$S(\hat{\mathcal{G}}, \mathcal{D}) = -\widehat{\text{MMD}}_k(\mathcal{D}, \hat{\mathcal{D}}) - \lambda|\hat{\mathcal{G}}|, \quad (3)$$

with  $|\hat{\mathcal{G}}|$  the number of edges in  $\hat{\mathcal{G}}$  and  $\widehat{\text{MMD}}_k$  defined as:

$$\frac{1}{n^2} \sum_{i,j=1}^n k(x_i, x_j) + \frac{1}{n^2} \sum_{i,j=1}^n k(\hat{x}_i, \hat{x}_j) - \frac{2}{n^2} \sum_{i,j=1}^n k(x_i, \hat{x}_j),$$

where kernel  $k$  usually is taken as the Gaussian kernel ( $k(x, x') = \exp(-\gamma\|x - x'\|_2^2)$ ). The MMD statistic, with quadratic complexity in the sample size, has the good property that it is zero if and only if  $P = \hat{P}$  as  $n$  goes to infinity [Gretton *et al.*, 2007]. For scalability, a linear approximation of the MMD statistics based on  $m$  random features [Lopez-Paz, 2016], called  $\widehat{\text{MMD}}_k^m$ , will also be used in the experiments. Due to the Gaussian kernel being differentiable,  $\widehat{\text{MMD}}_k$  and  $\widehat{\text{MMD}}_k^m$  are differentiable, and backpropagation can be used to learn the CGNN made of networks  $\hat{f}_i$  structured along  $\hat{\mathcal{G}}$ .

It is shown that the distribution  $\hat{P}$  of the CGNN can estimate the true observational distribution of the (unknown) FCM up to an arbitrary precision, under the assumption of an infinite observational sample:

**Proposition 3.** *Let  $\mathcal{D}$  be an infinite observational sample generated from  $(\mathcal{G}, f, \mathcal{E})$ . With same notations as in Prop. 2, for every  $\epsilon > 0$ , there exists a set  $\hat{f}_\epsilon = (\hat{f}_1, \dots, \hat{f}_d)$  such that the MMD between  $\mathcal{D}$  and an infinite size sample  $\hat{\mathcal{D}}_\ell$  generated from  $(\mathcal{G}, \hat{f}_\epsilon, \mathcal{E})$  is less than  $\epsilon$ .*

*Proof.* According to Prop. 2 and with same notations, letting  $\epsilon_\ell > 0$  go to 0 as  $\ell$  goes to infinity, consider  $\hat{f}_\ell = (\hat{f}_1^\ell, \dots, \hat{f}_d^\ell)$  and  $\hat{z}_\ell$  defined from  $\hat{f}_\ell$  such that for all  $e \in [0, 1]^d$ ,  $\|z(e) - \hat{z}_\ell(e)\| < \epsilon_\ell$ .

Let  $\{\hat{\mathcal{D}}_\ell\}$  denote the infinite sample generated after  $\hat{f}_\ell$ . The score of the CGNN  $(\mathcal{G}, \hat{f}_\ell, \mathcal{E})$  is  $\widehat{\text{MMD}}_k(\mathcal{D}, \hat{\mathcal{D}}_\ell) = \mathbb{E}_{e, e'}[k(z(e), z(e')) - 2k(z(e), \hat{z}_\ell(e')) + k(\hat{z}_\ell(e), \hat{z}_\ell(e'))]$ .

As  $\hat{f}_\ell$  converges towards  $f$  on the compact  $[0, 1]^d$ , using the bounded convergence theorem on a compact subset of  $\mathbb{R}^d$ ,  $\hat{z}_\ell(e) \rightarrow z(e)$  uniformly for  $\ell \rightarrow \infty$ , it follows from the

Gaussian kernel function being bounded and continuous that  $\widehat{\text{MMD}}_k(\mathcal{D}, \hat{\mathcal{D}}_\ell) \rightarrow 0$ , when  $\ell \rightarrow \infty$ .  $\square$

CGNN benefits from i) the representational power of generative networks to exploit distributional asymmetries; ii) the overall approximation of the joint distribution of the observational data to exploit conditional independences, to handle bivariate and multivariate causal modeling.

### 3.3 Searching causal graphs with CGNNs

The exhaustive exploration of all DAGs with  $d$  variables is super-exponential in  $d$ , preventing the use of brute-force methods for observational causal discovery even for moderate  $d$ . Following [Tsamardinos *et al.*, 2006; Nandy *et al.*, 2015], we assume known skeleton for  $\mathcal{G}$ , obtained via domain knowledge or a feature selection algorithm [Yamada *et al.*, 2014] under standard assumptions such as causal Markov, faithfulness, and sufficiency. Given a skeleton on  $X$  and the regularized MMD score (3), CGNN follows a greedy procedure to find  $\mathcal{G}$  and  $f_i$ :

- Orient each  $X_i - X_j$  as  $X_i \rightarrow X_j$  or  $X_j \rightarrow X_i$  by selecting the associated 2-variable CGNN with best score.
- Follow paths from a random set of nodes until all nodes are reached. Edges pointing towards a visited node reveal cycles, so must be reversed.
- For a number of iterations, reverse the edge that leads to the maximum improvement of the score  $S(\mathcal{G}, \mathcal{D})$  over a  $d$ -variable CGNN, without creating a cycle.

At the end of this process, we evaluate a confidence score for any edge  $X_i \rightarrow X_j$  as:

$$V_{X_i \rightarrow X_j} = S(\mathcal{G}, \mathcal{D}) - S(\mathcal{G} - \{X_i \rightarrow X_j\}, \mathcal{D}). \quad (4)$$

### 3.4 Dealing with hidden confounders

The search method above relies on the causal sufficiency assumption (no confounders). We relax this assumption as follows. Assuming confounders, each edge  $X_i - X_j$  in the skeleton is due to one out of three possibilities: either  $X_i \rightarrow X_j$ ,  $X_j \leftarrow X_i$ , or there exists an unobserved variable  $E_{i,j}$  such that  $X_i \leftarrow E_{i,j} \rightarrow X_j$ . Therefore, each equation in the FCM is extended to:  $X_i \leftarrow f_i(X_{\text{Pa}(i;\mathcal{G})}, E_{i, \text{Ne}(i;\mathcal{S})}, E_i)$ , where  $\text{Ne}(i;\mathcal{S}) \subset \{1, \dots, d\}$  is the set of indices of the variables adjacent to  $X_i$  in the skeleton. Each  $E_{i,j} \sim \mathcal{E}$  represents the hypothetical unobserved common causes of  $X_i$  and  $X_j$ . For instance, hiding  $X_1$  from the FCM in Fig. 1 would require considering a confounder  $E_{2,3}$ . Finally, when considering hidden confounders, the above third search step considers three possible mutations of the graph: reverse, add, or remove an edge. In this case,  $\lambda|\hat{\mathcal{G}}|$  promotes simple graphs.

## 4 Experiments

CGNN is empirically validated and compared to the state of the art on observational causal discovery of i) cause-effect relations (Section 4.2); ii) v-structures (Section 4.3); iii) multivariate causal structures with no confounders (Section 4.4); iv) multivariate causal structures when relaxing the no-confounder assumption (Section 4.5).

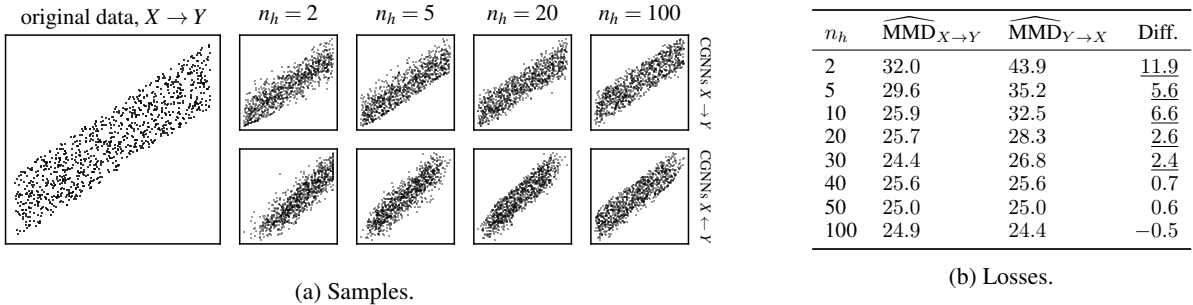


Figure 2: Samples and MMDs for CGNN models of different complexities (number of neurons) modeling the causal direction  $X \rightarrow Y$  (top row) and the anticausal direction  $X \leftarrow Y$  (bottom row) of a simple example. MMDs are averaged over 32 runs, underlined numbers indicate statistical significance at  $p = 10^{-3}$ .

#### 4.1 Experimental setting

MMD uses a sum of Gaussian kernels with bandwidths  $\gamma \in \{0.005, 0.05, 0.25, 0.5, 1, 5, 50\}$ . CGNN uses one-hidden-layer neural networks with  $n_h$  ReLU units, trained with the Adam optimizer [Kingma and Ba, 2014] and initial learning rate of 0.01, with full batch size  $n = 1500$ . The generated data involved from noise variables are sampled anew in each step. Each CGNN is trained for  $n_{\text{train}} = 1000$  epochs and evaluated on  $n_{\text{eval}} = 500$  generated samples. Reported results are averaged over 32 runs for  $\widehat{\text{MMD}}_k^m$  (resp. 64 runs for  $\widehat{\text{MMD}}_k^m$ ). All experiments run on an Intel Xeon 2.7GHz CPU, and an NVIDIA GTX 1080Ti GPU.

The most sensitive CGNN hyper-parameter is the number of hidden units  $n_h$ , governing the CGNN ability to model the causal mechanisms  $f_i$ : too small  $n_h$ , and data patterns may be missed; too large  $n_h$ , and overly complicated causal mechanisms might be retained. Overall,  $n_h$  is problem-dependent, as illustrated on a toy problem where two bivariate CGNNs are learned with  $n_h = 2, 5, 20, 100$  (Fig. 2.a) from data generated by FCM:  $X \sim \text{Uniform}[-2, 2], Y \leftarrow X + \text{Uniform}[0, 0.5]$ . Fig. 2.b shows the associated MMDs averaged on 32 independent runs, and confirms the importance of cross-validating model capacity [Zhang and Hyvärinen, 2009].

#### 4.2 Discovering cause-effect relations

Under the causal sufficiency assumption, the statistical dependence between two random variables  $X$  and  $Y$  is either due to causal relation  $X \rightarrow Y$  or  $X \leftarrow Y$ . The CGNN cause-effect accuracy is the fraction of edges in the graph skeleton that are rightly oriented, with Area Under Precision/Recall curve (AUPR) as performance indicator.

Five cause-effect inference datasets, covering a wide range of associations, are used. *CE-Cha* contains 300 cause-effect pairs from the challenge of [Guyon, 2013]. *CE-Net* contains 300 artificial cause-effect pairs generated using random distributions as causes, and neural networks as causal mechanisms. *CE-Gauss* contains 300 artificial cause-effect pairs as generated by [Mooij et al., 2016], using random mixtures of Gaussians as causes, and Gaussian process priors as causal mechanisms. *CE-Multi* contains 300 artificial cause-effect pairs built with random linear and polynomial causal mechanisms. In this dataset, we simulate additive or multiplicative

noise, applied before or after the causal mechanism. *CE-Tüb* contains the 99 real-world scalar cause-effect pairs from the Tübingen dataset [Mooij et al., 2016], concerning domains such as climatology, finance, and medicine. We set  $n \leq 1500$ .

The baseline and competitor methods<sup>2</sup> include: i) the Additive Noise Model ANM [Mooij et al., 2016], with Gaussian process regression and HSIC independence test; ii) the Linear Non-Gaussian Additive Model LiNGAM [Shimizu et al., 2006], a variant of Independent Component Analysis to identify linear causal relations; iii) The Information Geometric Causal Inference IGCI [Daniusis et al., 2012], with entropy estimator and Gaussian reference measure; iv) the Post-Non-Linear model PNL [Zhang and Hyvärinen, 2009], with HSIC test; v) The GPI method [Stegle et al., 2010], where the Gaussian process regression with higher marginal likelihood is selected as causal direction; vi) the Conditional Distribution Similarity statistic CDS [Fonollosa, 2016], which prefers the causal direction with lowest variance of conditional distribution variances; vii) the award-winning method Jarfo [Fonollosa, 2016], a random forest classifier trained on the ChaLearn Cause-effect pairs and hand-crafted to extract 150 features, including methods ANM, IGCI, CDS, and LiNGAM. For each baseline and competitor method, a leave-one-dataset-out scheme is used to select the best hyperparameters for each method (details omitted for brevity).

As shown in Table 1, i) linear regression methods are dominated; ii) CDS and IGCI perform well in some cases (e.g. when the entropy of causes is lower than those of effects); iii) ANM performs well when the additive noise assumption holds; iv) PNL, a generalization of ANM, compares favorably to the above methods; v) Jarfo performs well on artificial data but badly on real examples. Lastly, generative methods GPI and CGNN ( $\widehat{\text{MMD}}_k^m$ ) perform well on most datasets, including the real-world cause-effect pairs CE-Tüb, in counterpart for a higher computational cost (resp. 32 min on CPU for GPI and 24 min on GPU for CGNN). Using the linear MMD approximation [Lopez-Paz, 2016], CGNN ( $\widehat{\text{MMD}}_k^m$ ) as explained in Section 3.2) reduces the cost by a factor of 5 without hindering the performance. Overall, CGNN demonstrates competitive performance on the cause-effect inference problem, where it

<sup>2</sup><https://github.com/ssamot/causality>

Table 1: Cause-effect relations: Area Under the Precision Recall curve on 5 benchmarks for the cause-effect experiments (weighted accuracy in parenthesis for Tüb)

method	Cha	Net	Gauss	Multi	Tüb
Best fit	56.4	77.6	36.3	55.4	58.4 (44.9)
LiNGAM	54.3	43.7	66.5	59.3	39.7 (44.3)
CDS	55.4	89.5	84.3	37.2	59.8 (65.5)
IGCI	54.4	54.7	33.2	80.7	60.7 (62.6)
ANM	66.3	85.1	88.9	35.5	53.7 (59.5)
PNL	73.1	75.5	83.0	49.0	68.1 (66.2)
Jarfo	<u>79.5</u>	<u>92.7</u>	85.3	94.6	54.5 (59.5)
GPI	67.4	88.4	<u>89.1</u>	65.8	66.4 (62.6)
CGNN ( $\widehat{\text{MMD}}_k$ )	73.6	89.6	82.9	<u>96.6</u>	<u>79.8</u> (74.4)
CGNN ( $\widehat{\text{MMD}}_k^m$ )	76.5	87.0	88.3	94.2	76.9 (72.7)

is necessary to discover distributional asymmetries.

### 4.3 Discovering v-structures

Considering random variables  $(A, B, C)$  with skeleton  $A - B - C$ , four causal structures are possible: the *chain*  $A \rightarrow B \rightarrow C$ , the *reverse chain*  $A \leftarrow B \leftarrow C$ , the *v-structure*  $A \rightarrow B \leftarrow C$ , and the *reverse v-structure*  $A \leftarrow B \rightarrow C$ . Note that the chain, the reverse chain, and the reverse v-structure are Markov equivalent, and therefore indistinguishable from each other using statistics alone. This section thus examines the CGNN ability to identify v-structures.

Let us consider an FCM with causal mechanisms  $f_i = \text{Identity}$  and Gaussian noise variables (e.g.,  $B \leftarrow A + E_B$ ,  $E_B \sim \mathcal{N}(0, 1)$ ). As the joint distribution of one cause and its effect is symmetrical, the bivariate methods used in the previous section do not apply and the conditional independences among all three variables must be taken into account.

The retained experimental setting trains a CGNN for every possible causal graph with skeleton  $A - B - C$ , and selects the one with minimal MMD. CGNN accurately discriminates the v-structures from the other ones (0.202, 0.180), with a significantly lower MMD (0.127) for the ground truth causal graph. This proof of concept shows the ability of CGNN to detect and exploit conditional independences among variables.

### 4.4 Discovering multivariate causal structures

Consider a random vector  $X = (X_1, \dots, X_d)$ . Our goal is to find the FCM of  $X$  under the causal sufficiency assumption. At this point, we will assume known skeleton, so the problem reduces to orienting every edge. To that end, all experiments provide all algorithms *the true graph skeleton*, so their ability to orient edges is compared in a fair way. This allows us to separate the task of orienting the graph from that of uncovering the skeleton.

**Results on artificial data** We draw 500 samples from 20 training artificial causal graphs and 20 test artificial causal graphs on 20 variables. Each variable has a number of parents uniformly drawn in  $[[0, 5]]$ ;  $f_i$ s are randomly generated polynomials involving additive/multiplicative noise.

We compare CGNN to the PC algorithm [Spirtes *et al.*, 2000], the score-based methods GES [Chickering, 2002], LiNGAM [Shimizu *et al.*, 2006], causal additive model (CAM) [Peters *et al.*, 2014] and with the pairwise methods ANM and Jarfo. For PC, we employ the better-performing, order-independent version of the PC algorithm proposed by [Colombo and Maathuis, 2014]. PC needs the specification of a conditional independence test. We compare PC-Gaussian, which employs a Gaussian conditional independence test on Fisher z-transformations, and PC-HSIC, which uses the HSIC conditional independence test with the Gamma approximation [Gretton *et al.*, 2005]. PC and GES are implemented in the *palg* package [Kalisch *et al.*, 2012].

All hyperparameters are set on the training graphs in order to maximize the Area Under the Precision/Recall score (AUPR). For the Gaussian conditional independence test and the HSIC conditional independence test, the significance level achieving best result on the training set are respectively 0.1 and 0.05. For GES, the penalization parameter is set to 3 on the training set. For CGNN,  $n_h$  is set to 20 on the training set. For CAM, the cutoff value is set to 0.001.

Table 2 (left) displays the performance of all algorithms obtained by starting from the exact skeleton on the test set of artificial graphs and measured from the AUPR (Area Under the Precision/Recall curve), the Structural Hamming Distance (SHD, the number of edge modifications to transform one graph into another) and the Structural Intervention Distance (SID, the number of equivalent two-variable interventions between two graphs) [Peters and Bühlmann, 2013].

CGNN obtains significant better results with SHD and SID compared to the other algorithms when the task is to discover the causal from the true skeleton. Constraints based method PC with powerful HSIC conditional independence test is the second best performing method. It highlights the fact that when the skeleton is known, exploiting the structure of the graph leads to good results compared to pairwise methods using only local information. However CGNN and PC-HSIC are the most computationally expensive methods, taking an average of 4 hours on GPU and 15 hours on CPU, respectively.

The robustness of the approach is validated by randomly perturbing 20% edges in the graph skeletons provided to all algorithms (introducing about 10 false edges over 50 in each skeleton). As shown on Table 2 (middle), and as could be expected, the scores of all algorithms are lower when spurious edges are introduced. Among the least robust methods are constraint-based methods; a tentative explanation is that they heavily rely on the graph structure to orient edges. By comparison pairwise methods are more robust because each edge is oriented separately. As CGNN leverages conditional independence but also distributional asymmetry like pairwise methods, it obtains overall more robust results when there are errors in the skeleton compared to PC-HSIC.

CGNN obtains overall good results on these artificial datasets. It offers the advantage to deliver a full generative model useful for simulation (while e.g., Jarfo and PC-HSIC only give the causality graph). To explore the scalability of the approach, 5 artificial graphs with 100 variables have been considered, achieving an AUPRC of  $85.5 \pm 4$ , in 30 hours of computation on four NVIDIA 1080Ti GPUs.

Table 2: Average (std. dev.) results for the orientation of 20 artificial graphs given true skeleton (left), artificial graphs given skeleton with 20% error (middle), and real protein network given true skeleton (right). \* denotes statistical significance at  $p = 10^{-2}$ .

method	Skeleton without error			Skeleton with 20% of error			Causal protein network		
	AUPR	SHD	SID	AUPR	SHD	SID	AUPR	SHD	SID
<i>Constraints</i>									
PC-Gauss	0.67 (0.11)	9.0 (3.4)	131 (70)	0.42 (0.06)	21.8 (5.5)	191.3 (73)	0.19 (0.07)	16.4 (1.3)	91.9 (12.3)
PC-HSIC	0.80 (0.08)	6.7 (3.2)	80.1 (38)	0.49 (0.06)	19.8 (5.1)	165.1 (67)	0.18 (0.01)	17.1 (1.1)	90.8 (2.6)
<i>Pairwise</i>									
ANM	0.67 (0.11)	7.5 (3.0)	135.4 (63)	0.52 (0.10)	19.2 (5.5)	171.6 (66)	0.34 (0.05)	8.6 (1.3)	85.9 (10.1)
Jarfo	0.74 (0.10)	8.1 (4.7)	147.1 (94)	0.58 (0.09)	20.0 (6.8)	184.8 (88)	0.33 (0.02)	10.2 (0.8)	92.2 (5.2)
<i>Score-based</i>									
GES	0.48 (0.13)	14.1 (5.8)	186.4 (86)	0.37 (0.08)	20.9 (5.5)	209 (83)	0.26 (0.01)	12.1 (0.3)	92.3 (5.4)
LiNGAM	0.65 (0.10)	9.6 (3.8)	171 (86)	0.53 (0.10)	20.9 (6.8)	196 (83)	0.29 (0.03)	10.5 (0.8)	83.1 (4.8)
CAM	0.69 (0.13)	7.0 (4.3)	122 (76)	0.51 (0.11)	15.6 (5.7)	175 (80)	0.37 (0.10)	8.5 (2.2)	78.1 (10.3)
CGNN ( $\widehat{MMD}_k^m$ )	0.77 (0.09)	7.1 (2.7)	141 (59)	0.54 (0.08)	20 (10)	179 (102)	0.68 (0.07)	5.7 (1.7)	56.6 (10.0)
CGNN ( $\widehat{MMD}_k$ )	<u>0.89*</u> (0.09)	<u>2.5*</u> (2.0)	<u>50.45*</u> (45)	<u>0.62</u> (0.12)	16.9 (4.5)	<u>134.0*</u> (55)	<u>0.74*</u> (0.09)	<u>4.3*</u> (1.6)	<u>46.6*</u> (12.4)

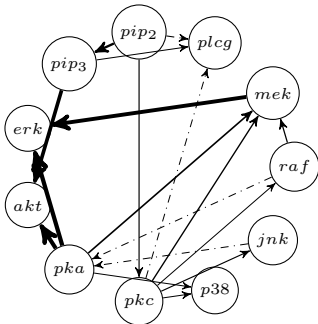


Figure 3: Causal protein network obtained with CGNN

**Results on real-world data** CGNN is applied to the protein network problem [Sachs *et al.*, 2005], using the Anti-CD3/CD28 dataset with 853 observational data points corresponding to general perturbations without specific interventions. All algorithms were given the skeleton of the causal graph [Sachs *et al.*, 2005, Fig. 2] with same hyper-parameters as in the previous subsection. We run each algorithm on 10-fold cross-validation. Table 2 (right) reports average (std. dev.) results.

Constraint-based algorithms obtain surprisingly low scores, because they cannot identify many V-structures in this graph. We confirm this by evaluating conditional independence tests for the adjacent tuples of nodes  $pip3-akt-pka$ ,  $pka-pmek-pkc$ ,  $pka-raf-pkc$  and we do not find strong evidences for V-structure. Therefore methods based on distributional asymmetry between cause and effect seem better suited to this dataset. CGNN obtains good results compared to the other algorithms. Notably, Figure 3 shows that CGNN is able to recover the strong signal transduction pathway  $raf \rightarrow mek \rightarrow erk$  reported in [Sachs *et al.*, 2005] and corresponding to clear direct enzyme-substrate causal effect. CGNN gives important scores for edges with good orientation (solid line), and low scores (thinnest edges) to the wrong edges (dashed line), suggesting that false causal discoveries may be controlled by using the confidence scores defined in Eq. (4).

#### 4.5 Dealing with hidden confounders

As real data often includes unobserved confounding variables, the robustness of CGNN is assessed by considering the previous artificial datasets while hiding some of the 20 observed variables in the graph. Specifically three random variables that cause at least two others in the same graph are hidden. Consequently, the skeleton now includes additional edges  $X - Y$  for all pairs of variables  $(X, Y)$  that are consequences of the same hidden cause (confounder). The goal in this section is to orient the edges due to direct causal relations, and to remove those due to confounders.

We compare CGNN to the RFCI algorithm (Gaussian or HSIC conditional independence tests) [Colombo *et al.*, 2012], which is a modification of the PC algorithm that accounts for hidden variables. For CGNN, we set the hyperparameter  $\lambda = 5 \times 10^{-5}$  fitted on the training graph dataset. Table 3 shows that CGNN is robust to confounders. Interestingly, true causal edges have high confidence, while edges due to confounding effects are removed or have low confidence.

Table 3: AUPR, SHD and SID on causal discovery with confounders. \* denotes significance at  $p = 10^{-2}$ .

method	AUPR	SHD	SID
RFCI-Gaussian	0.22 (0.08)	21.9 (7.5)	174.9 (58.2)
RFCI-HSIC	0.41 (0.09)	17.1 (6.2)	124.6 (52.3)
Jarfo	0.54 (0.21)	20.1 (14.8)	98.2 (49.6)
CGNN ( $\widehat{MMD}_k$ )	<u>0.71*</u> (0.13)	<u>11.7*</u> (5.5)	<u>53.55*</u> (48.1)

## 5 Conclusion

We introduced CGNN, a new framework to learn functional causal models from observational data based on generative neural networks. CGNNs minimize the maximum mean discrepancy between their generated samples and the observed data. CGNNs combines the power of deep learning and the interpretability of causal models. Once trained, CGNNs are causal models of the world able to simulate the outcome of interventions. Future work includes i) extending the proposed approach to categorical and temporal data, ii) characterizing sufficient identifiability conditions for the approach, and iii) improving the computational efficiency of CGNN.

## References

- [Carlier *et al.*, 2016] Guillaume Carlier, Victor Chernozhukov, and Alfred Galichon. Vector quantile regression beyond correct specification. *arXiv*, 2016.
- [Chickering, 2002] David Maxwell Chickering. Optimal structure identification with greedy search. *JMLR*, 2002.
- [Colombo and Maathuis, 2014] Diego Colombo and Marloes H Maathuis. Order-independent constraint-based causal structure learning. *JMLR*, 2014.
- [Colombo *et al.*, 2012] Diego Colombo, Marloes H Maathuis, Markus Kalisch, and Thomas S Richardson. Learning high-dimensional directed acyclic graphs with latent and selection variables. *The Annals of Statistics*, 2012.
- [Cybenko, 1989] George Cybenko. Approximation by superpositions of a sigmoidal function. *Mathematics of Control, Signals, and Systems (MCS)*, 2(4):303–314, 1989.
- [Danušis *et al.*, 2012] Povilas Daniušis, Dominik Janzing, Joris Mooij, Jakob Zscheischler, Bastian Steudel, Kun Zhang, and Bernhard Schölkopf. Inferring deterministic causal relations. *arXiv*, 2012.
- [Fonollosa, 2016] José Fonollosa. Conditional distribution variability measures for causality detection. *arXiv*, 2016.
- [Goodfellow *et al.*, 2016] Ian Goodfellow, Yoshua Bengio, and Aaron Courville. *Deep Learning*. MIT Press, 2016. <http://www.deeplearningbook.org>.
- [Gretton *et al.*, 2005] Arthur Gretton, Ralf Herbrich, Alexander Smola, Olivier Bousquet, and Bernhard Schölkopf. Kernel methods for measuring independence. *JMLR*, 2005.
- [Gretton *et al.*, 2007] Arthur Gretton, Karsten M Borgwardt, Malte Rasch, Bernhard Schölkopf, Alexander J Smola, et al. A kernel method for the two-sample-problem. *NIPS*, 2007.
- [Guyon, 2013] Isabelle Guyon. Chalearn cause effect pairs challenge, 2013.
- [Hoyer *et al.*, 2009] Patrik O Hoyer, Dominik Janzing, Joris M Mooij, Jonas Peters, and Bernhard Schölkopf. Non-linear causal discovery with additive noise models. *NIPS*, 2009.
- [Kalisch *et al.*, 2012] Markus Kalisch, Martin Mächler, Diego Colombo, Marloes H Maathuis, Peter Bühlmann, et al. Causal inference using graphical models with the r package pcalg. *Journal of Statistical Software*, 2012.
- [Kingma and Ba, 2014] Durk P Kingma and Jimmy Ba. Adam: A Method for Stochastic Optimization. *ICLR*, 2014.
- [Li *et al.*, 2015] Yujia Li, Kevin Swersky, and Richard S Zemel. Generative moment matching networks. *ICML*, 2015.
- [Lopez-Paz *et al.*, 2015] David Lopez-Paz, Krikamol Muandet, Bernhard Schölkopf, and Ilya O Tolstikhin. Towards a learning theory of cause-effect inference. *ICML*, 2015.
- [Lopez-Paz, 2016] David Lopez-Paz. *From dependence to causation*. PhD thesis, University of Cambridge, 2016.
- [Mooij *et al.*, 2016] Joris M Mooij, Jonas Peters, Dominik Janzing, Jakob Zscheischler, and Bernhard Schölkopf. Distinguishing cause from effect using observational data: methods and benchmarks. *JMLR*, 2016.
- [Nandy *et al.*, 2015] Preetam Nandy, Alain Hauser, and Marloes H Maathuis. High-dimensional consistency in score-based and hybrid structure learning. *arXiv*, 2015.
- [Pearl, 2003] Judea Pearl. Causality: models, reasoning and inference. *Econometric Theory*, 2003.
- [Pearl, 2009] Judea Pearl. *Causality*. 2009.
- [Peters and Bühlmann, 2013] Jonas Peters and Peter Bühlmann. Structural intervention distance (sid) for evaluating causal graphs. *arXiv*, 2013.
- [Peters *et al.*, 2014] Jonas Peters, Joris M Mooij, Dominik Janzing, and Bernhard Schölkopf. Causal discovery with continuous additive noise models. *The Journal of Machine Learning Research*, 15(1):2009–2053, 2014.
- [Peters *et al.*, 2017] Jonas Peters, Dominik Janzing, and Bernhard Schölkopf. *Elements of Causal Inference - Foundations and Learning Algorithms*. MIT Press, 2017.
- [Sachs *et al.*, 2005] Karen Sachs, Omar Perez, Dana Pe’er, Douglas A Lauffenburger, and Garry P Nolan. Causal protein-signaling networks derived from multiparameter single-cell data. *Science*, 308(5721):523–529, 2005.
- [Shimizu *et al.*, 2006] Shohei Shimizu, Patrik O Hoyer, Aapo Hyvärinen, and Antti Kerminen. A linear non-gaussian acyclic model for causal discovery. *JMLR*, 2006.
- [Spirtes *et al.*, 2000] Peter Spirtes, Clark N Glymour, and Richard Scheines. *Causation, prediction, and search*. MIT Press, 2000.
- [Stegle *et al.*, 2010] Oliver Stegle, Dominik Janzing, Kun Zhang, Joris M Mooij, and Bernhard Schölkopf. Probabilistic latent variable models for distinguishing between cause and effect. *NIPS*, 2010.
- [Stock and Cisse, 2017] P. Stock and M. Cisse. ConvNets and ImageNet Beyond Accuracy: Explanations, Bias Detection, Adversarial Examples and Model Criticism. *arXiv*, 2017.
- [Tsamardinos *et al.*, 2006] Ioannis Tsamardinos, Laura E Brown, and Constantin F Aliferis. The max-min hill-climbing bayesian network structure learning algorithm. *Machine learning*, 2006.
- [Yamada *et al.*, 2014] Makoto Yamada, Wittawat Jitkrittum, Leonid Sigal, Eric P Xing, and Masashi Sugiyama. High-dimensional feature selection by feature-wise kernelized lasso. *Neural computation*, 2014.
- [Zhang and Hyvärinen, 2009] Kun Zhang and Aapo Hyvärinen. On the identifiability of the post-nonlinear causal model. *UAI*, 2009.